

# Data-based Fault Detection and Isolation Using Output Feedback Control <sup>\*</sup>

Benjamin J. Ohran <sup>\*</sup> Jinfeng Liu <sup>\*</sup>  
David Muñoz de la Peña <sup>\*\*\*</sup> Panagiotis D. Christofides <sup>\*,\*\*,1</sup>  
James F. Davis <sup>\*</sup>

<sup>\*</sup> *Department of Chemical and Biomolecular Engineering, University of California, Los Angeles, CA 90095-1592 USA.*

<sup>\*\*</sup> *Department of Electrical Engineering, University of California, Los Angeles, CA 90095-1592, USA.*

<sup>\*\*\*</sup> *Departamento de Ingeniería de Sistemas y Automática, Universidad de Sevilla, Camino de los Descubrimientos S/N, 41092, Sevilla, Spain.*

---

**Abstract:** This work focuses on data-based fault detection and isolation (FDI) of nonlinear process systems. Working within the framework of controller-enhanced fault detection and isolation that we recently introduced, we address and solve an unresolved, practical problem. We consider the case where only output measurements are available and design appropriate state estimator-based output feedback controllers to achieve controller-enhanced fault detection and isolation in the closed-loop system. The necessary conditions for achieving fault detection and isolation using output feedback control are provided. We use a nonlinear chemical process example to demonstrate the applicability and effectiveness of the proposed method.

*Keywords:* Process control, process monitoring, state estimation, fault detection and isolation

---

## 1. INTRODUCTION

Advanced automation technology has changed how the chemical process industry operates in many ways. Over the last few decades, advancements in plant operations have led to higher efficiency and improved economics through better control and monitoring of process systems. These technological advances have resulted in process systems becoming increasingly automated, no longer requiring operators to open and close valves in order to manually perform process control. In general, there is a trend towards such “smart” plants that are capable of highly automated control with decision making at the plant level taking into account environmental, health, safety and economic considerations (Christofides et al. (2007)). With increased amounts of sensors and actuators, it becomes possible to design systems capable of detecting and handling process or control system abnormalities through fault-tolerant control (FTC) (see for example, Mhaskar et al. (2006, 2007)). This is an important area of research as abnormal situations cost U.S. industries over \$20 billion each year (Nimmo (1995)). A key element of a successful FTC system is a fast, accurate method for detecting faulty process behavior and isolating its cause. The fault detection and isolation (FDI) problem is the focus of the present work.

In a previous work (Ohran et al. (2008)), we developed an FDI method that takes advantage of both model-based and data-based approaches. This method brought together elements of model-based controller design and statistical pro-

cess monitoring. In this method, the controller is designed with the FDI scheme in mind in addition to stability and performance criteria. By enforcing an isolable structure in the closed-loop system, it becomes possible to perform FDI based on statistical evaluation of process measurements. The purpose of the present work is to further develop the approach proposed in Ohran et al. (2008) by relaxing the requirement of full state feedback control. Specifically, we consider the case where only output measurements are available and design appropriate state estimator-based output feedback controllers to achieve controller-enhanced fault detection and isolation in the closed-loop system. This is demonstrated using a nonlinear chemical process example to show the applicability and effectiveness of the proposed method.

## 2. PRELIMINARIES

### 2.1 Process system structure

We consider nonlinear process systems with the following general state-space description:

$$\dot{x} = f(x, u, d) \quad (1)$$

where  $x \in \mathbb{R}^n$  is the vector of process state variables,  $u \in \mathbb{R}^m$  is the vector of manipulated input variables and  $d \in \mathbb{R}^p$  is the vector of  $p$  possible actuator faults or disturbances. Vector  $d$  is equal to zero when the system is under normal operating conditions. When fault  $k$ , with  $k = 1, \dots, p$  occurs,  $d_k$  can take any time-varying value. The approach of controller enhanced FDI was introduced in Ohran et al. (2008) as a method of dividing the state vector into a number of partially decoupled subvectors. These subvectors can be monitored using measured process data.

---

<sup>\*</sup> Financial support from NSF, CTS-0529295, is gratefully acknowledged.

<sup>1</sup> Corresponding author: P.D. Christofides, pdc@seas.ucla.edu

Based on their responses and the system structure enforced by the decoupling controller, it is possible to discriminate between individual faults or groups of faults. In order to understand the necessary structure to perform isolation, we review the definitions of the incidence graph, the reduced incidence graph and the isolability graph (Ohran et al. (2008)).

*Definition 1.* The incidence graph of the system of Eq.1 is a directed graph defined by  $n$  nodes, one for each state,  $x_i$ ,  $i = 1 \dots n$ , of the system. A directed arc with origin in node  $x_i$  and destination in node  $x_j$  exists if and only if  $\frac{\partial f_j}{\partial x_i} \neq 0$ .

The arcs in the incidence graph illustrate dependencies within the states of the system. A path through more than one arc that starts and ends at the same node is denoted as a loop.

*Definition 2.* The reduced incidence graph of the system of Eq.1 is the directed graph of  $N$  nodes, one for each  $q_i$ ,  $i = 1 \dots N$ , where  $N$  is the maximum number of nodes that satisfy the following conditions:

- Each node  $q_i$  corresponds to a set of states  $X_i = \{x_j\}$ . These sets of states are a partition of the state vector of the system, i.e.,  

$$\bigcup X_i = \{x_1, \dots, x_n\}, \quad X_i \cap X_j = \emptyset, \quad \forall i \neq j.$$
- A directed arc with origin  $q_i$  and destination  $q_j$  exists if and only if  $\frac{\partial f_l}{\partial x_k} \neq 0$  for some  $x_l \in X_i$ ,  $x_k \in X_j$ .
- There are no loops in the graph.

The reduced incidence graph reveals the partially decoupled subsystems within the structure of the states in  $x$ .

*Definition 3.* The isolability graph of the system of Eq.1 is a directed graph made of the  $N$  nodes of the reduced incidence graph and  $p$  additional nodes, one for each possible fault  $d_k$ . In addition, a directed arc with origin in fault node  $d_k$  and destination to a state node  $q_j$  exists if and only if  $\frac{\partial f_i}{\partial d_k} \neq 0$  for some  $x_l \in X_j$ .

These definitions present the basic dependencies within a state vector. In most nonlinear process systems, the states are fully coupled and the isolability graph contains a single node representing all of the states in the system. However, in systems with partially decoupled dynamics these figures demonstrate graphically the subsets of the state vector.

With the isolability graph of a system, we can perform fault isolation based upon monitoring the subsystems. For this purpose, it is necessary to review the definition of a fault signature given below (Ohran et al. (2008)):

*Definition 4.* The signature of a fault  $d_k$  of the system of Eq.1 is a binary vector  $W^k$  of dimension  $N$ , where  $N$  is the number of nodes of the reduced incidence graph of the system. The  $i^{th}$  component of  $W^k$ , denoted  $W_i^k$ , is equal to 1 if there exists a path in the isolability graph from the node corresponding to fault  $d_k$  to the node  $q_i$  corresponding to the set of states  $X_i$ , or 0 otherwise.

## 2.2 Process monitoring

For the purpose of monitoring whether or not a state has deviated from its normal behavior, we use statistical process monitoring methods. Specifically, we use Hotelling's

$T^2$  statistic developed in Hotelling (1947), a well established method in statistical process control that monitors multivariate normal (Gaussian) data using a single statistic. Because of its suitability for continuous, serially correlated chemical processes, the method of using single observations is employed (Tracy et al. (1992)). Given a multivariate state vector  $x$  of dimension  $n$ , the  $T^2$  statistic can be computed using the mean  $\bar{x}$  and the estimated covariance matrix  $S$  of process data obtained under normal operating conditions (see, for example, Kourti and MacGregor (1996)), as follows:

$$T^2 = (x - \bar{x})^T S^{-1} (x - \bar{x}). \quad (2)$$

The upper control limit (UCL) for the  $T^2$  statistic can be calculated from its distribution, under the assumption that the data are multivariate normal, according to the following formula:

$$T_{UCL}^2 = \frac{(h^2 - 1)n}{h(h - n)} F_\alpha(n, h - n) \quad (3)$$

where  $h$  is the number of historical measurements used in estimating  $S$ ,  $F_\alpha(n, h - n)$  is the value on the  $F$  distribution with  $(n, h - n)$  degrees of freedom for which there is probability  $\alpha$  of a greater or equal value occurring.

In order to perform FDI, the  $T^2$  statistic based on the full state vector  $x$  with upper control limit  $T_{UCL}^2$  is first used to detect the presence of a fault. Subsequently, the  $T_i^2$  statistic is used to monitor the status of each subset of the state vector with an upper control limit  $T_{UCLi}^2$  where  $i = 1, \dots, N$  that is based on each of the subvectors and their states  $x_j \in X_i$ . The fault detection and isolation procedure then follows the steps given below (Ohran et al. (2008)):

1. A fault is detected if  $T^2(t) > T_{UCL}^2 \forall t_f \leq t \leq t_f + T_P$  where  $t_f$  is last time when  $T^2$  crossed the UCL and  $T_P$  is the fault detection window chosen. Choosing  $T_P$  depends on the process time constants and on historical information of past process behavior.
2. Fault isolation can be performed by comparing fault signatures with the process signature  $W(t_f, T_P)$  which can be built as follows:

$$\begin{aligned} T_i^2(t) > T_{UCLi}^2 \forall t_f \leq t \leq t_f + T_P &\rightarrow W_i(t_f, T_P) = 1. \\ T_i^2(t) \not> T_{UCLi}^2 \forall t_f \leq t \leq t_f + T_P &\rightarrow W_i(t_f, T_P) = 0. \end{aligned}$$

A fault  $d_k$  is isolated at time  $t_f + T_P$  if  $W(t_f, T_P) = W^k$ . If two or more faults are defined by the same signature, further isolation between them is not possible on the basis of the fault signature.

## 2.3 Controller design for enhanced FDI

*Decoupling controller design* The approach to fault detection and isolation discussed in the previous section can be applied if the signatures of the faults in the closed-loop system are distinct. The uniqueness of a fault depends on the structure of the closed-loop system and the faults considered. In general, complex nonlinear systems are fully coupled (i.e., cannot be broken down into partially decoupled subvectors). However, an isolable structure in the closed-loop system may still be achieved through the application of appropriately designed nonlinear control laws. As an example, consider a controller that can be

applied to nonlinear systems with the following state space description:

$$\begin{aligned}\dot{x}_1 &= f_{11}(x_1) + f_{12}(x_1, x_2) + g_1(x_1, x_2)u + d_1 \\ \dot{x}_2 &= f_2(x_1, x_2) + d_2\end{aligned}\quad (4)$$

where  $x_1 \in R$ ,  $x_2 \in \mathbb{R}^n$ ,  $u \in \mathbb{R}$  and  $g_1(x_1, x_2) \neq 0$  for all  $x_1 \in R$ ,  $x_2 \in \mathbb{R}^n$ . With a nonlinear state feedback controller of the form:

$$u(x_1, x_2) = -\frac{f_{12}(x_1, x_2) - v(x_1)}{g_1(x_1, x_2)} \quad (5)$$

the closed-loop system takes the form

$$\begin{aligned}\dot{x}_1 &= f_{11}(x_1) + v(x_1) + d_1 \\ \dot{x}_2 &= f_2(x_1, x_2) + d_2\end{aligned}\quad (6)$$

where  $v(x_1)$  has to be designed in order to achieve asymptotic stability of the origin of the  $x_1$  subsystem when  $d_1 = 0$ . In this case, the controller of Eq.5 guarantees asymptotic stability of the closed-loop system, as well as different signatures for faults  $d_1$  and  $d_2$ . For more detailed results, see Ohran et al. (2008).

*Input/output linearizable nonlinear systems* Input/output linearizable nonlinear systems constitute a special class of nonlinear systems for which it is possible to systematically design nonlinear controllers to achieve controller-enhanced fault detection and isolation. Using a feedback-linearizing control law that takes the following general form,

$$u(x) = \frac{1}{L_g L_f^{r-1} h(x)} [v(x) - L_f^r h(x)] \quad (7)$$

where  $L_f^r h(x)$  is the  $r$ -th order Lie derivative,  $L_g L_f^{r-1} h(x)$  is a mixed Lie derivative and  $v(x)$  is an external controller for the purpose of stabilizing the system, the system under closed loop operation will have linear input-output dynamics.

If the state-feedback law given in Eq.7 is applied to an input/output linearizable system, faults affecting the system can be isolated into two different groups: those that affect the output and those that do not affect the output. The induced structure of the closed-loop system provides different signatures for the faults depending on the relative degree of the output with respect to the fault and the relative degree of the output with respect to the input. Faults with relative degree higher than the relative degree of the input will not affect the output. Thus, when a fault occurs, taking into account whether the trajectory of the output has deviated from the normal case or not, it is possible to isolate to which group the fault belongs. For the definitions of relative degree and an in depth discussion of feed-back linearization in this context, see Ohran et al. (2008).

### 3. CONTROLLER ENHANCED FDI USING OUTPUT FEEDBACK CONTROL

#### 3.1 State estimation

In order to perform controller enhanced FDI using output feedback control, any unknown process state variable must be quickly and accurately estimated from the available output measurements so that the decoupling state feedback controller designs of subsections 2.3.1 and 2.3.2 can be implemented. The state estimation is performed for

the state vector  $x$  (or a subset thereof) with the outputs, or measured states, defined as  $y = Cx$ . In this work, we consider only outputs of the form  $y_i = x_i$ ,  $i = 1, \dots, q < n$ . In other words,  $C$  is a matrix with one and only one non-zero entry in each row and that entry is equal to unity. This set-up is appropriate in chemical process control applications where measurements of a few states like temperature and concentrations of a few species, like key products, are available, but concentrations of some species are not measured. This set-up also allows obtaining a clear picture of the use of output feedback instead of full state feedback in controller enhanced FDI. The theory for the state estimator design is based upon a linear system, but can also be applied to nonlinear systems, using a local stability analysis around the operating point (origin). Specifically, the linearized model of the nonlinear system of Eq.1 takes the following form:

$$\begin{aligned}\dot{x} &= Ax + Bu + Wd \\ y &= Cx\end{aligned}\quad (8)$$

where  $A$  is the Jacobian matrix of the nonlinear system at the operating point,  $u$  is the manipulated input vector and  $d$  is the fault vector. The matrices  $B$  and  $W$  can be computed from the linearization of Eq.1 around the origin. Under the assumption that  $(A, C)$  forms an observable pair, each state variable  $x$  can be estimated by the following dynamic equation:

$$\dot{\hat{x}} = A\hat{x} + Bu + L(y - C\hat{x}) \quad (9)$$

where  $\hat{x}$  is the state estimate and  $L$  is the estimator gain that can be chosen so that all the eigenvalues of the matrix  $(A - LC)$  are placed at appropriate locations in the left-half of the complex plane to guarantee a desirable rate of convergence of the estimation error to zero. The computation of  $L$  can be done using standard pole placement techniques or via a Kalman filtering framework by adding process and measurement noise in the linearized model of Eq.8. In either case, the linearized state estimation error equation with  $d(t) = 0$  takes the form:

$$\dot{e} = (A - LC)e. \quad (10)$$

where  $e = x - \hat{x}$  is the estimation error. While it is possible to perform state estimation using the full state vector in the state estimator of Eq.9 when  $d(t) \equiv 0$ , it becomes necessary to use a reduced-order process model when designing a state estimator-based output feedback controller to enhance FDI. This need for a reduced-order model arises due to faults that affect the state estimator and introduce error into the estimate (i.e., the full state estimation scheme of Eq.9 works when  $d(t) = 0$ , but not when  $d(t) \neq 0$ ). Specifically, if the error vector  $d$  on the right-hand side of Eq.8 is nonzero, the new equation for the estimator error becomes  $\dot{e} = (A - LC)e + Wd$ . Thus, in the presence of a fault, the state estimates no longer converge to their actual values, and the isolable structure attained in the closed-loop system under state feedback control cannot be maintained. However, it is possible in some process systems to perform the state estimation task using a subset of the states that are not directly affected by the expected faults, i.e., effectively eliminating  $d$  in the estimation error system. The general structure of the model in Eqs.8-10 remains the same for the reduced-order system, but it is based on a subset of the full state vector,  $x_r \subset x$ . To mathematically realize this notion, consider a system with the following structure, where time derivatives of the states

$x_r$  are not functions of  $d$  and include all unknown states to be estimated along with some measured states, and  $x_d$  includes the remaining measured states, whose dynamic equations may be functions of  $d$ . Specifically, we consider the following decomposition of the vectors and matrices of the linearized system of Eq.8

$$\begin{aligned} x &= \begin{bmatrix} x_r \\ x_d \end{bmatrix}, \quad A = \begin{bmatrix} A_r & A_{rd} \\ A_{dr} & A_d \end{bmatrix}, \quad W = \begin{bmatrix} 0 \\ W_d \end{bmatrix} \\ B &= \begin{bmatrix} B_r \\ B_d \end{bmatrix}, \quad C = \begin{bmatrix} C_r & 0 \\ 0 & C_d \end{bmatrix}, \quad y = \begin{bmatrix} y_r \\ y_d \end{bmatrix}. \end{aligned} \quad (11)$$

Provided that the pair  $(A_r, C_r)$  is observable, the state estimator based on the reduced-order system then takes the form:

$$\dot{\hat{x}}_r = A_r \hat{x}_r + A_{rd} x_d + B_r u + L_r (y_r - C_r \hat{x}_r) \quad (12)$$

Eq.12 uses the actual measured values for all of the states in  $x_d$ . We can break  $x_r$  down further into measured states and unmeasured states,  $x_r = [x_{rm}^T \ x_{ru}^T]^T$ . Note that  $x_{rm}$  must include enough measured states independent of  $d$  for the system to be observable. Given the restrictions on  $C$ , this implies that  $y_r = C_r x_r = x_{rm}$  and  $C_d = I$  (i.e.,  $y_d = x_d$ ). Finally, we define a vector with full state information by combining the measured and estimated data,  $\hat{x} = [x_{rm}^T \ \hat{x}_{ru}^T \ x_d^T]^T$ . Note that  $\hat{x}_{rm}$  is only used as the driving force for convergence of the state estimator. With these definitions, the reduced-order state estimator of Eq.12 is not a direct function of  $d$  and the dynamics of the estimation error,  $e_r = x_r - \hat{x}_r$ , take the form  $\dot{e}_r = (A_r - L_r C_r) e_r$  which implies that  $e_r(t)$  will converge to zero even in the presence of a change in  $d$ .

Once the estimator gain obtained from the linearized model of the system is calculated, it can then be used to estimate the states of the process using the nonlinear model dynamics. Once again, for the nonlinear system, the state vector,  $x$ , decomposes into the one of the reduced-order system (independent of  $d$ ) and the remaining states, i.e.,  $x = [x_r^T \ x_d^T]^T$  and  $f([x_r^T \ x_d^T]^T, u, d) = [f_r(x_r, x_d, u)^T \ f_d(x_r, x_d, u, d)^T]^T$ . The nonlinear dynamic equations for the reduced-order system are then combined with the estimator gain and the output error to create a nonlinear state estimator as follows:

$$\dot{\hat{x}}_r = f_r(\hat{x}_r, x_d, u) + L_r (y_r - h_r(\hat{x}_r)) \quad (13)$$

where the measured values are used for the states in  $x_d$ , i.e., by assumption  $y_d = x_d$ . Note that following the previous assumption,  $h_r(x_r) = C_r x_r$ . Combining the nonlinear state estimator of Eq.13 with a nonlinear state feedback controller,  $u = p_{DC}(x)$ , that enforces an isolable structure in the closed-loop system and can be designed following the approaches presented in subsections 2.3.1 and 2.3.2, we obtain the following dynamic nonlinear output feedback controller:

$$\begin{aligned} \dot{\hat{x}}_r &= f_r(\hat{x}_r, x_d, p_{DC}(\hat{x})) + L_r (y_r - C_r \hat{x}_r) \\ u &= p_{DC}(\hat{x}) \end{aligned} \quad (14)$$

Due to the effect of estimation error, it is not possible to achieve complete decoupling. However, it is possible to achieve a near isolable structure that is sufficient for practical purposes. In this sense, we consider a near isolable structure to be one where the closed-loop system under output feedback control can be seen as an  $O(e_r)$  regular perturbation of the closed-loop system under state

feedback control which is locally exponentially stable and has an isolable structure. Thus, the estimation error can be viewed a small perturbation error that will be accounted for by the FDI thresholds designed to filter out normal process variation. Theorem 1 below summarizes the main analysis and controller design result of this section as well as the closed-loop FDI properties.

*Theorem 1.* Consider the closed-loop system of Eq.1 under the nonlinear output feedback controller of Eq.14 and assume that the pair  $(A_r, C_r)$  is observable and  $L_r$  is designed such that the matrix  $(A_r - L_r C_r)$  has all of its eigenvalues in the left-half of the complex plane. Then, there exist  $\delta, \epsilon$  and  $T_y$  such that if  $f$  is continuously differentiable on  $D = \{x \in \mathbb{R}^n \mid \|x\|_2 < \delta\}$ , the Jacobian of  $f$  is bounded and Lipschitz on  $D$  and  $\max\{\|x(t_0)\|_2, \|\hat{x}_r(t_0)\|_2\} < \delta$  then  $\|x_r(t) - \hat{x}_r(t)\|_2 < \epsilon, \forall t > t_0 + T_y$ , and a near isolable structure is enforced in the closed-loop system.

**Proof.** Under the control law of Eq.14, the closed-loop system of Eq.1 takes the form,

$$\begin{aligned} \dot{x} &= f(x, p_{DC}(\hat{x}), d), \quad y = h(x) \\ \dot{\hat{x}}_r &= f_r(\hat{x}_r, x_d, p_{DC}(\hat{x})) + L_r (y_r - h_r(\hat{x}_r)). \end{aligned} \quad (15)$$

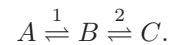
Linearizing the closed-loop system of Eq.15 around the equilibrium point (origin) yields,

$$\begin{aligned} \dot{x} &= Ax + B p_{DC}(\hat{x}), \quad y = Cx \\ \dot{\hat{x}}_r &= A_r \hat{x}_r + A_{rd} x_d + B_r p_{DC}(\hat{x}) + L_r (y_r - C_r \hat{x}_r). \end{aligned} \quad (16)$$

The error between the actual and estimated states of the reduced-order, linearized system is then  $e_r = x_r - \hat{x}_r$  with the dynamics  $\dot{e}_r = (A_r - L_r C_r) e_r$ . Assuming that the pair  $(A_r, C_r)$  is observable and that  $L_r$  is chosen such that the matrix  $A_r - L_r C_r$  has eigenvalues in the left-half of the complex plane, the estimation error,  $e_r$ , in the linearized system has exponentially stable dynamics. If the vector field of the nonlinear system,  $f(x, p_{DC}(\hat{x}), d)$ , is continuously differentiable and the Jacobian matrix is bounded and Lipschitz on  $D = \{x \in \mathbb{R}^n \mid \|x\|_2 < \delta\}$ , then the nonlinear system dynamics are also locally, exponentially stable within some region around the equilibrium point Khalil (1992). For some initial condition  $\max\{\|x_0\|_2, \|x_{r0}\|_2\} < \delta$ , the state estimation error,  $e_r$ , will be bounded such that  $\|x_r - \hat{x}_r\| < \epsilon \forall t > t_0 + T_y$ , where  $T_y$  is a time interval of  $O(\epsilon)$ . Thus, the output feedback control approaches state feedback control with error of order  $\epsilon$ , i.e.,  $x_r = \hat{x}_r + O(\epsilon) \forall t > t_0 + T_y$ . For sufficiently small  $\epsilon$ , this leads to a near isolable structure in the closed-loop system for almost all times since the state feedback controller  $p_{DC}(x)$  enforces an isolable structure in the closed-loop system.

### 3.2 Application to a CSTR example

The example considered is a well-mixed CSTR in which a feed component  $A$  is converted to an intermediate species  $B$  and finally to the desired product  $C$ , according to the reaction scheme



Both steps are elementary, reversible reactions and are governed by the following Arrhenius relationships:

$$r_1 = k_{10}e^{-\frac{E_1}{RT}}C_A, \quad r_{-1} = k_{-10}e^{-\frac{E_{-1}}{RT}}C_B \quad (18)$$

$$r_2 = k_{20}e^{-\frac{E_2}{RT}}C_B, \quad r_{-2} = k_{-20}e^{-\frac{E_{-2}}{RT}}C_C \quad (19)$$

where  $k_{i0}$  is the pre-exponential factor and  $E_i$  is the activation energy of the  $i^{th}$  reaction where the subscripts 1, -1, 2, -2 refer to the forward and reverse reactions of steps 1 and 2.  $R$  is the gas constant, while  $C_A$ ,  $C_B$  and  $C_C$  are the molar concentrations of species  $A$ ,  $B$  and  $C$ , respectively. The feed to the reactor consists of pure  $A$  at flow rate  $F$ , concentration  $C_{A0}$  and temperature  $T_0$ . The state variables of the system include the concentrations of the three main components  $C_A$ ,  $C_B$ , and  $C_C$  as well as the temperature of the reactor,  $T$ . Using first principles and standard modeling assumptions, the following mathematical model of the process is obtained

$$\begin{aligned} \dot{C}_A &= \frac{F}{V}(C_{A0} - C_A) - r_1 + r_{-1} + d_1 \\ \dot{C}_B &= -\frac{F}{V}C_B + r_1 - r_{-1} - r_2 + r_{-2} \\ \dot{C}_C &= -\frac{F}{V}C_C + r_2 - r_{-2} \\ \dot{T} &= \frac{F}{V}(T_0 - T) + \frac{(-\Delta H_1)}{\rho c_p}(r_1 - r_{-1}) \\ &\quad + \frac{(-\Delta H_2)}{\rho c_p}(r_2 - r_{-2}) + u + d_2 \end{aligned} \quad (20)$$

where  $V$  is the reactor volume,  $\Delta H_1$  and  $\Delta H_2$  are the enthalpies of the first and second reactions, respectively,  $\rho$  is the fluid density,  $c_p$  is the fluid heat capacity,  $u = Q/\rho c_p$  is the manipulated input, where  $Q$  is the heat input to the system,  $d_1$  denotes a disturbance in the inlet concentration and  $d_2$  denotes a fault in the control actuator. The system of Eq.20 is modeled with sensor measurement noise and autoregressive process noise. For details on noise generation and for complete system parameter values, please refer to Ohran et al. (2008).

In order to obtain the estimated trajectory for  $C_B$ , a state estimator as in Eq.13 was implemented using the reduced-order system  $\hat{x}_r = [\hat{C}_B \ \hat{C}_C]^T$ . The process measurements for  $C_A$  and  $T$  were used in computing the dynamics of  $\hat{x}_r$ . Note that although  $C_C$  is measured, it is used in the reduced-order state estimator so that the reduced-order system is observable. The control input was updated at each sampling interval with the measured values for  $C_A$ ,  $T$  and  $C_C$  and the estimated value of  $\hat{C}_B$ . As discussed in subsection 3.1,  $C_A$  and  $T$  should not be modeled as dynamic states in the estimator since they are directly affected by the faults  $d_1$  and  $d_2$ . Thus, the measured data for  $C_A$  and  $T$  must be used in modeling the estimator, and the final form of the state estimator based on the reduced subsystem  $\hat{x}_r = [\hat{C}_B \ \hat{C}_C]^T$  is as given below:

$$\begin{aligned} \dot{\hat{C}}_B &= -\frac{F}{V}\hat{C}_B + r_1 - r_{-1} - r_2 + r_{-2} + L_1(C_C - \hat{C}_C) \\ \dot{\hat{C}}_C &= -\frac{F}{V}\hat{C}_C + r_2 - r_{-2} + L_2(C_C - \hat{C}_C) \end{aligned} \quad (21)$$

with

$$r_1 = k_{10}e^{-\frac{E_1}{RT}}C_A, \quad r_{-1} = k_{-10}e^{-\frac{E_{-1}}{RT}}\hat{C}_B$$

$$r_2 = k_{20}e^{-\frac{E_2}{RT}}\hat{C}_B, \quad r_{-2} = k_{-20}e^{-\frac{E_{-2}}{RT}}\hat{C}_C$$

where  $L$  is the filter gain obtained using Kalman-filtering theory based on the reduced-order system. The resulting value for  $L_r$  is  $[L_{r1} \ L_{r2}]^T = [0.0081 \ 0.0559]^T$ .

The controlled output of the system, for the purpose of feedback linearization, is defined as the concentration of the desired product  $y = h(x) = C_C$  (although, the measured output vector is  $y_m = [C_A \ T \ C_C]^T$ .) We consider only faults  $d_1$  and  $d_2$ , which represent undesired changes in  $C_{A0}$  (disturbance) and  $Q$  (actuator fault), respectively. In this process, the manipulated input  $u$  appears in the temperature dynamics and the output,  $y = C_C$ , has relative degree 2 with respect to  $u$ . The fault  $d_1$  appears only in the dynamics of  $C_A$  and the output,  $y = C_C$ , has relative degree 3 with respect to  $d_1$ . Finally, the output has relative degree 2 with respect to  $d_2$ . Based on the relative degrees of the output with respect to the input and with respect to the faults, under feedback linearizing control the system structure will be such that the state vector can be separated into two subsets:  $X_1 = \{C_A, \hat{C}_B, T\}$  and  $X_2 = \{C_C\}$ . Thus, the fault signature for  $d_1 = [1 \ 0]^T$  and for  $d_2 = [1 \ 1]^T$ . During the simulation, the  $T^2$  for the full state vector is monitored in order to perform fault detection (substituting the estimate  $\hat{C}_B$  for the unknown state  $C_B$ .) Each of the subsystems is monitored to compute the system signature upon detection of a fault. Based on observation of the system dynamic behavior, a fault detection window,  $T_P$ , of 1 min is used.

The control objective is to regulate the system at the equilibrium point

$$\begin{aligned} C_{As} &= 2.06 \frac{\text{kmol}}{\text{m}^3}, \quad C_{Bs} = 1.00 \frac{\text{kmol}}{\text{m}^3}, \quad C_{Cs} = 0.937 \frac{\text{kmol}}{\text{m}^3}, \\ T_s &= 312.6\text{K}, \quad u_s = 0\text{K/s} \end{aligned} \quad (22)$$

where the subscript  $s$  refers to the steady state values of the variables. It should be noted that the CSTR system of Eq.20 belongs to the class of systems of Eq.1 with  $x = [C_A - C_{As}, \ T - T_s, \ C_B - C_{Bs}, \ C_C - C_{Cs}]^T$  where  $C_B$  is replaced with  $\hat{C}_B$  in the definition of  $\hat{x}$ . This implies that we can apply the output feedback scheme presented using the controlled output  $y = C_C$ . Using Eq.7, the feedback-linearizing controller takes the following form:

$$u = \frac{v - L_f^2 h(\hat{x})}{L_g L_f h(\hat{x})} \quad (23)$$

with

$$v = [-2\zeta_1 - 2\zeta_2].$$

where

$$\begin{aligned} \zeta_1 &= C_C, \quad \zeta_2 = -\frac{F}{V}C_C + r_2 - r_{-2} \\ r_2 &= k_{20}e^{-\frac{E_2}{RT}}\hat{C}_B, \quad r_{-2} = k_{-20}e^{-\frac{E_{-2}}{RT}}C_C. \end{aligned}$$

The state variables are in the transformed space and are shifted so that the origin represents the desired set-point.

The closed-loop system was simulated for each of the two faults considered. Each simulation was run for a process time of 1 hour with the fault occurring at  $t = 40 \text{ min}$ . The values for the faults were each zero prior to the fault

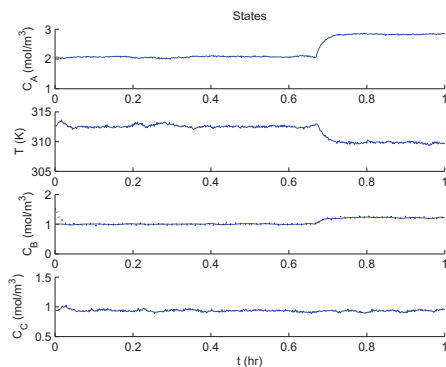


Fig. 1. Plot of measured state values for the CSTR under output feedback decoupling control with fault  $d_1$ .  $C_B$  shows both actual (solid) and estimated (dotted) values.

occurring and took constant values of  $d_1 = 1 \text{ kmol}/\text{m}^3\text{min}$  and  $d_2 = 10 \text{ K}/\text{min}$  at  $t = 40 \text{ min}$ . The state estimator was initialized far from the operating point at  $\hat{C}_B(0) = 1.5 \text{ kmol}/\text{m}^3$  and  $\hat{C}_C(0) = C_C(0) = C_{C_s}$  in order to demonstrate convergence.

Figure 1 shows the trajectories for each of the states in the simulation with a failure in  $d_1$ . The fault is apparent at approximately  $t = 40 \text{ min}$  ( $0.667\text{hr}$ ). We can readily see from the state trajectories, that the decoupling scheme was effective as evidenced by the fact that the output,  $C_C$ , is unaffected by the fault. Also, we see that the state estimator converged at around  $t = 3 \text{ min}$ .

For the system with a failure in  $d_1$ , Figure 2 shows the Hotelling's  $T^2$  statistic for the two subvectors  $X_1$  and  $X_2$  as well as for the full state vector. From the graph, we can see that a fault is clearly detected at the expected time  $t = 40 \text{ min}$  as shown in the plot of the  $T^2$  statistic for the full state vector ( $T_3^2$ ). Although there were a few single incidents of data breaching the upper control limit, none of them represented sustained departures for the length of the fault detection window,  $T_P$ . Also note that values above the upper control limit before  $t = 0.1\text{hr}$  were due to the state estimator not having converged. Upon detection of the fault, the system signature can be computed as  $W = [1 \ 0]^T$  due to the fact that the  $T^2$  statistic for the subvector  $X_1$  exceeded the upper control limit for a sustained period and the  $T^2$  for the subvector  $X_2$  remained within the bounds of normal operation. Because the system signature matches that of the fault signature for  $d_1$ , a fault in  $d_1$  is declared at time  $t \approx 41 \text{ min}$ . In Figure 3, we see the simulation results for the same system with a failure in  $d_2$ . Again, the failure is evident around  $t = 40 \text{ min}$ . However, in this case we see that both subsystems are affected. The process signature obtained from the  $T^2$  statistics in Figure 3 shows that both subvectors were affected and this process signature matches the fault signature of  $d_2$ .

## REFERENCES

- Christofides, P.D., Davis, J.F., El-Farra, N.H., Clark, D., Harris, K.R.D., and Gipson, J.N. (2007). Smart plant operations: Vision, progress and challenges. *AIChE Journal*, 53, 2734–2741.
- Hotelling, H. (1947). Multivariate quality control. In O. Eisenhart (ed.), *Techniques of Statistical Analysis*,

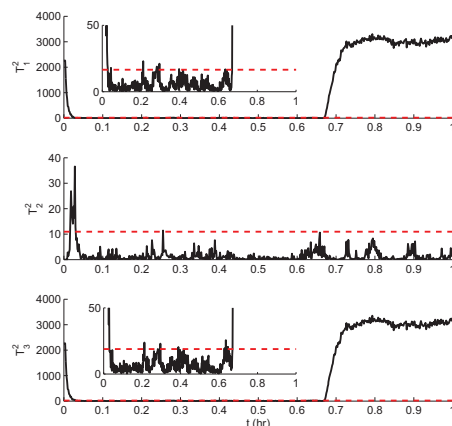


Fig. 2.  $T^2$  statistics for the CSTR under output feedback decoupling control with fault  $d_1$  for the subsystem  $X_1$  ( $T_1^2$ ), the subsystem  $X_2$  ( $T_2^2$ ) and the full system  $x$  ( $T_3^2$ ).

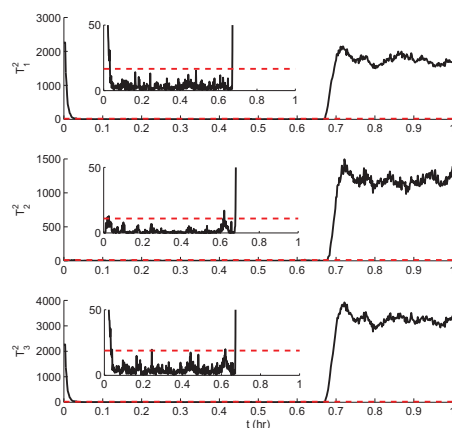


Fig. 3.  $T^2$  statistics for the CSTR under output feedback decoupling control with fault  $d_2$  for the subsystem  $X_1$  ( $T_1^2$ ), the subsystem  $X_2$  ( $T_2^2$ ) and the full system  $x$  ( $T_3^2$ ).

113–184. McGraw-Hill.

- Khalil, H. (1992). *Nonlinear Systems*. Macmillan Publishing Company.
- Kourti, T. and MacGregor, J. (1996). Multivariate SPC methods for process and product monitoring. *Journal of Quality Technology*, 28, 409–428.
- Mhaskar, P., Gani, A., and Christofides, P.D. (2006). Fault-tolerant process control: Performance-based re-configuration and robustness. *International Journal of Robust & Nonlinear Control*, 16, 91–111.
- Mhaskar, P., Gani, A., McFall, C., Christofides, P.D., and Davis, J.F. (2007). Fault-tolerant control of nonlinear systems subject to sensor data losses. *AIChE Journal*, 53, 654–668.
- Nimmo, I. (1995). Adequately address abnormal operations. *Chem. Eng. Prog.*, 91, 36–45.
- Ohran, B.J., Muñoz de la Peña, D., Christofides, P.D., and Davis, J.F. (2008). Enhancing data-based fault isolation through nonlinear control. *AIChE Journal*, 54, 223–241.
- Tracy, N.D., Young, J.C., and Mason, R.L. (1992). Multivariate control charts for individual observations. *Journal of Quality Technology*, 24, 88–95.